Available online at www.sciencedirect.com
ScienceDirect
Ceramics International 34 (2008) 853–857
CERAMICS INTERNATIONAL
www.elsevier.com/locate/ceramint

Phase change and electrical resistivity of Zn–Mn–Ni–O-based NTC thermistors produced using IZC powder recycled from used dry batteries

J. Takahashi [a,*], A. Miura [a], H. Itoh [b], K. Sawayama [c], T. Akazawa [c], K. Nebuka [d], H. Miura [e], M. Kishi [f]

[a] Division of Materials Chemistry, Graduate School of Engineering, Hokkaido University, N-13 W-8 Kita-ku, Sapporo 060-8628, Japan
[b] Department of Materials Science, Kitami Institute of Technology, Kitami 090-8507, Japan
[c] Department of Materials Technology, Hokkaido Industrial Research Institute, Sapporo 060-0819, Japan
[d] Hokkai Spring MFG Co., Otaru 047-0261, Japan
[e] Nomura Kosan Co., Tokyo 103-0012, Japan
[f] Hokkaido Institute of Technology, Sapporo 006-8585, Japan

Available online 29 September 2007

Abstract

Zn–Mn–Ni–Oxide-based NTC thermistors with variable Ni/Mn ratios were fabricated from powder mixtures of recycled IZC, and commercial $MnCO_3$ and $NiCO_3$. Solid phases and electrical resistivity of each sintered sample were studied as a function of Ni/Mn ratio, sintering temperature and sintering time. At 1200 °C for 2 h, samples with the Ni/Mn ratios of 0.38 and higher were found to consist of cubic spinel as a major phase. After sintering at 1250 °C for 10 h, densification proceeded with a phase change from cubic spinel to tetragonal one. The electrical resistivity of the samples obtained at 1200 °C for 2 h progressively decreased with an increasing Ni/Mn ratio up to 0.38, at which the value became the lowest (4.2×10^3 Ω cm at room temperature) of all the samples fabricated.

Keywords: A. Sintering; C. Electrical conductivity; D. Spinels; E. Thermistors

1. Introduction

In modern life, dry batteries are extensively used with increasing development of a variety of electronic devices. For example, more than five billion industrial and household batteries have been annually produced in Japan since 2000. Up to now, however, the recycling of used dry batteries is very limited, although several recycling methods have been explored [1–3] and reusable inorganic or metal resources are actually produced from them in Japan. This current situation predominantly resulted from limited practical applications of such recycled materials [4–6].

Itomuka zinc calcine (IZC) is one of the reusable materials, which is a powder consisting of the oxides of zinc and manganese as a major constituent. A specialized research project has been started under financial support of Hokkaido Industrial Research Institute to promote the recycling of the used dry batteries and to expand the practical usage of the recycled powder, IZC. The present authors have also started an intensive study focusing on the development of practical functional ceramics. In the previous study, the single-phase spinel solid solutions of $ZnMn_2O_4$ were synthesized from mixtures of calcined IZC and different amounts of Mn-source material [5]. In addition, NTC thermistors with an appropriate value of electrical resistivity and B-constant were obtained when a small amount of NiO was added to the synthesized $ZnMn_2O_4$-type spinels. In general, NTC thermistors are widely used and required to have a variety of resistivity, depending on their applications. Therefore, in order to produce IZC-based practical NTC thermistors with a wide range of electrical resistivity, bulk samples having controlled Ni/Mn ratios were fabricated by solid-state powder processing of the mixtures of IZC, Mn- and Ni-carbonates. Changes of solid phases, spinel

* Corresponding author. Tel.: +81 11 706 6572; fax: +81 11 706 6572.
E-mail address: tkjun@eng.hokudai.ac.jp (J. Takahashi).

0272-8842/$34.00
doi:10.1016/j.ceramint.2007.09.035

Table 1
Mixing ratio and the corresponding element ratio of starting powders

Sample	IZC (g)	Mn[a](g)	Ni[a](g)	Corresponding element ratio[b]			
				Zn	Mn	Ni	Ni/Mn
7-Ni	20.00	9.60	2.90	30	63	7	0.11
13-Ni	20.00	6.93	5.58	31	56	13	0.23
19-Ni	20.00	4.45	8.05	31	50	19	0.38
24-Ni	20.00	2.11	10.36	31	45	24	0.53
30-Ni	20.00	0.0	12.50	31	39	30	0.77

[a] Commercial carbonate powders.
[b] XRF analysis.

composition and electrical resistivity were investigated as a function of the Ni/Mn ratio and sintering conditions.

2. Experimental procedure

The IZC powder was calcined at 900 °C for 4 h and then washed repeatedly with distilled water to substantially reduce the concentrations of K, S and Cl components from as-received IZC powder, which were deteriorative effect on the densification of IZC powder [5]. Fixed amounts of the treated-IZC and commercial Mn- and Ni-carbonates were mixed by wet ball-milling in a plastic container for 24 h to prepare starting powders with different compositions shown in Table 1 where the mass-based mixing ratio and the corresponding element ratio determined by X-ray fluorescence analysis (XRF) are given. These mixed powders were calcined at 900 °C for 4 h in air. Green compacts of calcined powders with variable Ni/Mn ratios were sintered at the temperatures ranging 1200–1250 °C for 2 or 10 h in air. X-ray powder diffractometry (XRD, Rigaku RINT-2000) and scanning electron microscopy (SEM, JEOL JSM-6300F and JSM-6500F with EDS analyzer) were used for solid phase identification and microstructural analysis of sintered samples, respectively. After coating both surfaces with Ag paste, the change in electrical resistivity of the sintered samples was measured using an LCR-meter (YHP-4274A) during cooling process from 500 °C.

3. Results and discussion

3.1. Phase change and structural refinement of cubic phase

Fig. 1 shows solid phases formed after heating at 1200 °C for 2 h for each sample. Both the 7-Ni and 13-Ni samples revealed substantially broadened peaks of the tetragonal $ZnMn_2O_4$ and $ZnMnO_3$-type phases. However, very sharpened profiles corresponding to the $ZnMnO_3$-type phase appeared for samples with higher Ni content, 19-Ni, 24-Ni and 30-Ni samples. There is little structure information on the $ZnMnO_3$-type phase. Because the components of Zn, Mn and Ni can occupy the two-fold and six-fold sites in the spinel structure [7,8], the $ZnMnO_3$-type phase detected in this study had been thought to be closely related to the spinel structure. The profile fitting with Rietveld analysis for the $ZnMnO_3$-type phase showed that it could be identified with cubic spinel phase. For the samples having 19 mol% Ni and more, some Mn^{3+} cations on the octahedral

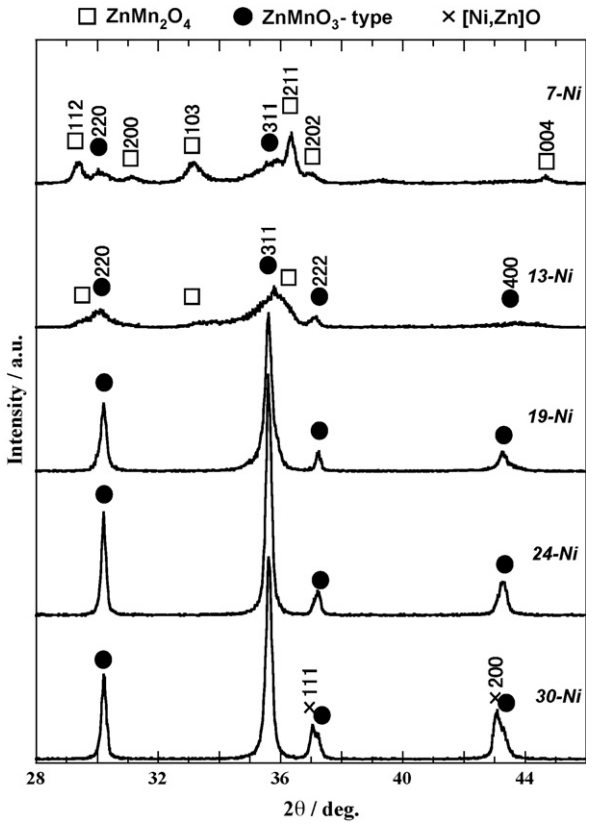

Fig. 1. XRD patterns of samples heated at 1200 °C for 2 h.

sites, for which Ni^{2+} cations were substituted, changed to Mn^{4+} cations by charge neutralization. The change $Mn^{3+} \rightarrow Mn^{4+}$ on the octahedral sublattice caused the formation of the cubic spinel phase due to the reduction of Jahn–Teller effect. The symmetry change from tetragonal to cubic in the spinel structure should be affected by the Mn^{3+}/Mn^{4+} ratio in the octahedral polyhedra. Fig. 2 shows the effect of heating

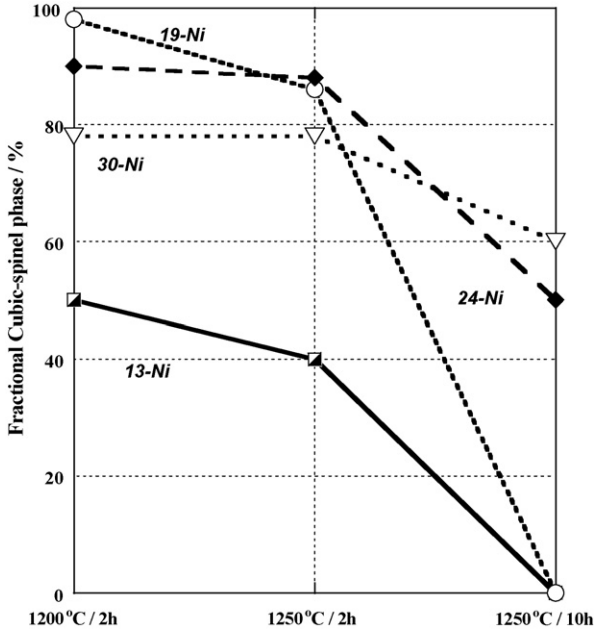

Fig. 2. Fractional cubic phase in each sample heated under different conditions.

temperature on the site occupancy of cations in the spinel structure, that is, the relative stability of the cubic spinel phase. For the 19-, 24-, and 30-Ni samples, the cubic spinel was the major solid phase up to 1250 °C for 2 h. After prolonged heating at 1250 °C, however, the cubic spinel completely changed into the tetragonal one for the 19-Ni sample.

In order to clarify the chemical composition of the spinel phases formed, an element analysis with EDS was conducted for each sample sintered at 1200 °C. The homogeneous distributions of Zn, Mn and Ni elements could be observed for the 19-Ni sample, indicating the formation of the single-phase of the cubic spinel. For the 24- and 30-Ni samples, however, Ni-enriched regions and the correspondingly Mn-poor regions were distributed as can be seen in Fig. 3. For the Zn–Mn–Ni-oxide spinel solid solutions, diversely different cationic distributions were reported [8], which would come from differences in synthesis process, thermal treatment and measuring technique for the cationic distribution. Table 2 shows the chemical compositions derived from EDS for the cubic spinel and NaCl-type NiO ss grains in each sample sintered at 1200 °C for 2 h. The mixing ratio of the starting mixtures changed such as an increase in the Ni content and the corresponding decrease in the Mn content from the 19-Ni to 30-Ni samples. Despite of the substantial composition change in the starting powders, the resulting cubic spinel phases in the 19-Ni–30-Ni samples were found to have slightly different cation ratios. Thus, the composition of the cubic spinel produced after heating at 1200 °C for 2 h for the 19-Ni sample could be approximated to be Zn:Mn:Ni ≈ 33:47:20. Based on the result obtained for $NiMn_2O_4$ spinel in which all the Ni^{2+} cations are located on the octahedral sites when the Ni content is lower than 0.66 [9], the cubic spinel of the 19-Ni sample might be formulated as $Zn^{2+}[Ni_{0.60}{}^{2+}Mn_{0.60}{}^{4+}\ Mn_{0.80}{}^{3+}]O_4$. Slightly

Table 2
Chemical compositions of cubic spinel and NiOss grains in each sample sintered at 1200 °C for 2 h

Compound	Sample	Composition (mol%)		
		Zn	Mn	Ni
Cubic spinel	19-Ni	33	47	20
	24-Ni	34	48	18
	30-Ni	36	47	17
NiO ss	19-Ni	9	5	86
	24-Ni	16	5	78
	30-Ni	28	5	67

higher Zn contents observed for the cubic spinels in the 24-Ni and 30-Ni samples probably caused the incorporation of a small fraction of Zn into the octahedral sublattice as described in the literature [8] with the simultaneous dissolution of some Ni^{2+} cations out of the sites. Different stability behaviors of the cubic spinel phase shown in Fig. 3 could be explained by this different site occupancy. That is, Zn cations on the octahedral sites might inhibit the reduction of Mn^{4+} to Mn^{3+} on the same sites at elevated temperature. Under heating at 1200 °C for 2 h, the relative amounts of the cubic phase and NiOss were estimated to be about 98:2, 90:10 and 78:22 for the 19-Ni, 24-Ni and 30-Ni samples, respectively.

3.2. Temperature dependence of resistivity

Bulk densities of the samples sintered under different conditions are revealed in Fig. 4. Comparing with the theoretical one of the $ZnMn_2O_4$ spinel (5.25 g/cm^3), considerably porous samples with about 80% of their theoretical density were produced at 1200 °C/2 h, whereas density increase

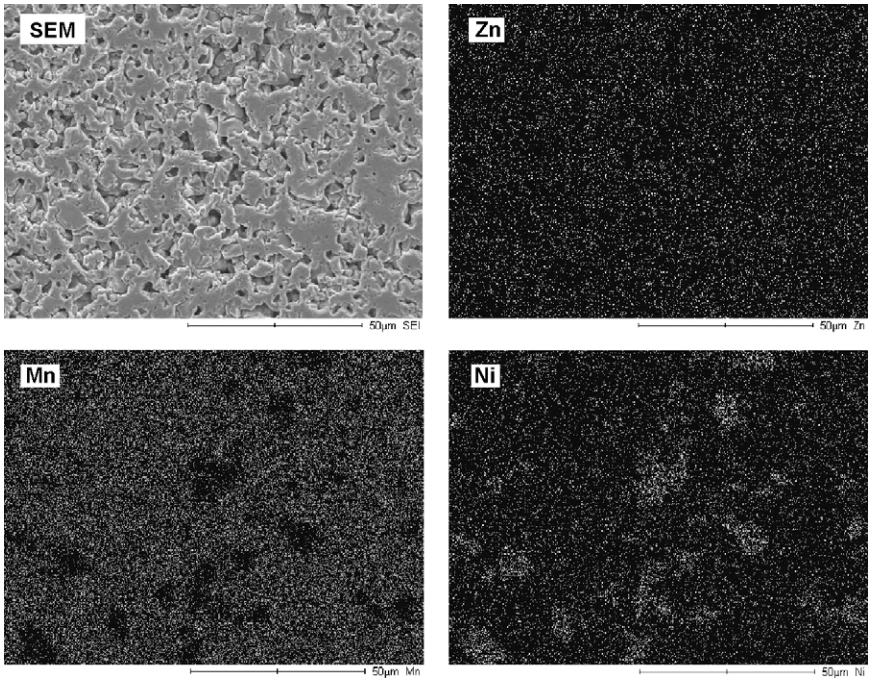

Fig. 3. Mappings of Zn, Ni and Mn elements for the 30-Ni sample sintered at 1200 °C for 2 h.

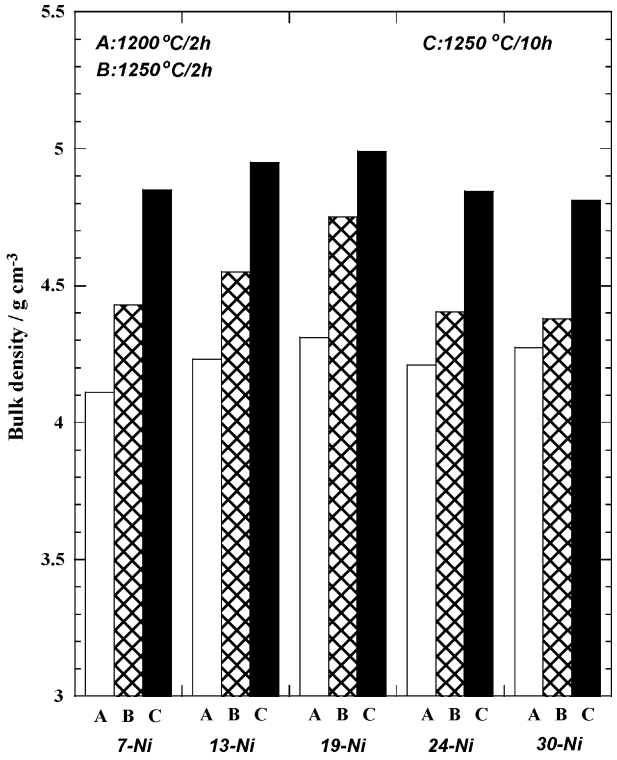

Fig. 4. Density changes of each sample sintered under different conditions.

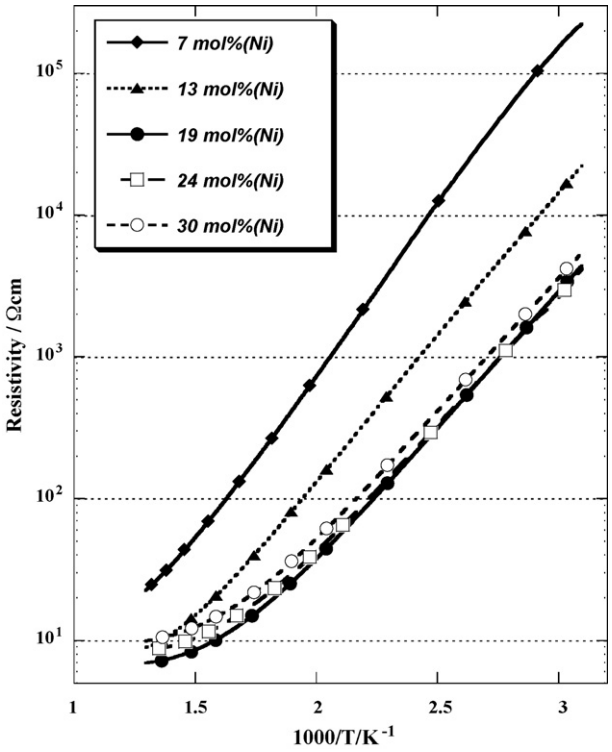

Fig. 5. Temperature dependence of resistivity for samples sintered at 1200 °C for 2 h.

with increasing temperature and prolonged heating was recognized for each sample having different compositions. Fig. 5 shows changes in the ac resistivity at 1 kHz with temperature up to 500 °C for those sintered at 1200 °C for 2 h. The values of the resistivity were strongly dependent on the Ni content over a wide temperature range, while maintaining the NTC characteristic in all the samples. Particularly, samples consisting of the cubic spinel phase indicated much lower values of resistivity. The conductive property of the 19-Ni, 24-Ni and 30-Ni samples could be explained by the electron hopping between Mn^{3+} and Mn^{4+} on the six-fold sublattice, for which Mn^{4+} was created by the Ni^{2+} substitution [10,11].

Relationship between structure change of the spinel phase and resistivity can be seen in Fig. 6 for the 19-Ni samples.

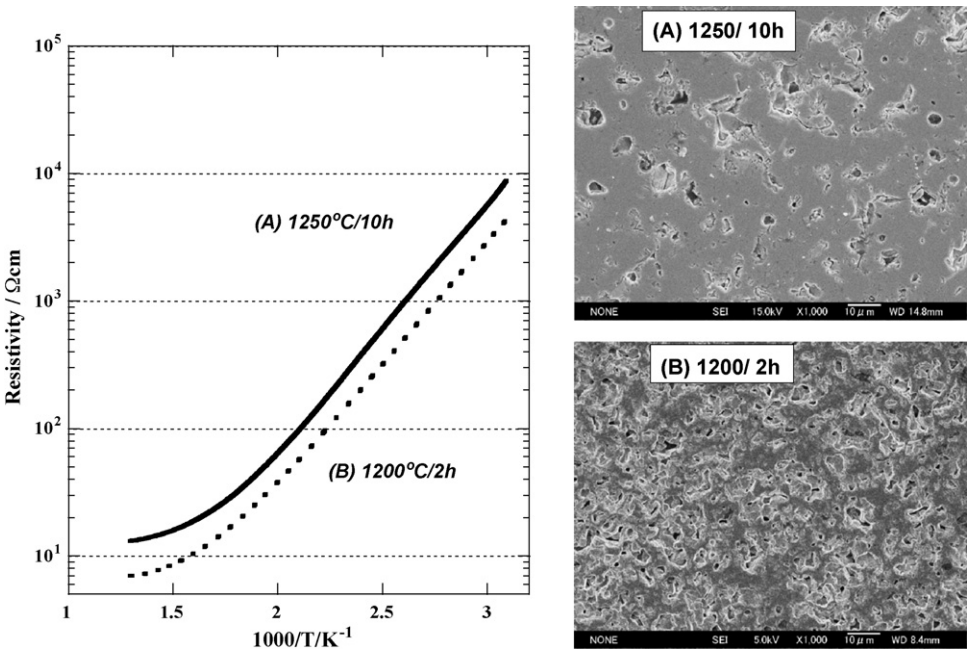

Fig. 6. Effect of spinel structure on the resistivity of (A) well-sintered and (B) poorly-sintered 19-Ni samples.

Different sintering conditions of 1200 °C/2 h and 1250 °C/10 h resulted in the production of bulk samples with considerably different density and structure symmetry. The resistivity of the 19-Ni-1250 °C/10 h sample is slightly higher over entire temperature range than that of the 19-Ni-1200 °C/2 h sample, despite that the densification after sintering was clearly promoted for the 19-Ni- 1250 °C/10 h sample as seen in the SEM images in Fig. 6. The composition of the tetragonal spinel in the 19-Ni-1250 °C/10h sample was estimated ton be Zn:Mn:Ni = 33:51:16, which was a Mn-rich and Ni-poor composition compared with that of the cubic spinel phase of the 19-Ni-1200 °C/2 h sample. Heating at higher temperature for prolonged duration caused the oxidation state of the Mn^{4+} cations on the six-fold sites to be reduced to Mn^{3+}, leading to the dissolution of some part of Ni^{2+} out of the spinel structure. Thus, higher resistivity of the 19-Ni-1250 °C/10 h sample might be attributed to the phase change of the spinel; the single cubic spinel phase of the 19-Ni-1200 °C/2h sample turned into mixed phases of the tetragonal spinel with a different composition and NiO ss. Stability test in which resistivity drift was checked in the temperature range from −30 to 80 °C indicated that elements fabricated from the 19-Ni-1200 °C/2 h sample was fairly stable, being comparable to the electrical property of commercially available NTC thermistors.

4. Conclusions

IZC-based NTC thermistors were fabricated from powder mixtures of recycled IZC, and commercial Mn- and Ni-carbonates. The $ZnMnO_3$-type phase produced in the bulk samples with more than 19 mol% Ni content (19-Ni, 24-Ni and 30-Ni) was refined by Rietveld analysis. It could be identified with the cubic spinel consisting of Mn^{3+}, Mn^{4+} and Ni^{2+} on the six-fold lattice sites. The composition of the cubic phase for the 19-Ni sample obtained at 1200 °C for 2 h was estimated to be $Zn^{2+}[Ni_{0.60}{}^{2+}Mn_{0.60}{}^{4+}\ Mn_{0.80}{}^{3+}]O_4$. The cubic spinel gradually changed to the tetragonal one with dissolution of some of the Ni constituent from spinel structure as sintering temperature was raised, which was due to the reduction of Mn^{4+} created by the Ni^{2+} substitution to Mn^{3+}. The electrical resistivity of the bulk samples sintered at 1200 °C for 2 h substantially decreased with an increasing Ni content up to the 19-Ni sample, which showed the lowest value of $\sim 4 \times 10^3\ \Omega$ cm at room temperature. The IZC-based NTC thermistors fabricated in this study were proved to have stable electrical property comparable to the commercial one.

References

[1] Y. Saotome, Y. Nakazawa, Y. Yamada, Disassembling and materials recovering process of alkaline manganese dry batteries by vacuum-aided recycling systems technology, Vacuum 53 (1999) 101–104.
[2] N. Vatistas, M. Bartolozzi, S. Arras, The dismantling of the spent alkaline zinc manganese dioxide batteries and the recovery of the zinc from the anodic material, J. Power Sources 101 (2001) 182–187.
[3] D.C.R. Espinosa, A.M. Bernardes, J.A.S. Tenorio, An overview on the current processes for the recycling of batteries, J. Power Sources 135 (2004) 311–319.
[4] J. Takahashi, T. Shigyo, S. Shimada, H. Itoh, M. Kishi, T. Akazawa, Fabrication and NTC characteristic of oxide spinel solid solutions containing Zn, Mn and Al from the waste of dead batteries, J. Ceram. Soc. Jpn. 110 (7) (2002) 681–687 (in Japanese).
[5] J. Takahashi, H. Itoh, M. Kishi, T. Akazawa, H. Miura, Formation and sintering characteristics of $ZnMn_2O_4$-type spinels using IZC powder recycled from the waste of used dry batteries, J. Ceram. Soc. Jpn. 112 (5) (2004) S1352–S1357.
[6] G.X. Xi, Y.Q. Li, Y.M. Liu, Study on preparation of manganese–zinc ferrites using spent Zn–Mn batteries, Mater. Lett. 58 (2004) 1164–1167.
[7] D.M. Adams, Inorganic Solids, John Wiley & Sons, New York, 1974 pp. 151–156.
[8] S.G. Uillemet-Fritsch, J.L. Baudour, C. Chanel, F. Bouree, A. Rousset, X-ray and neutron diffraction studies on nickel zinc manganite $Mn_{2.35-x}Ni_{0.65}Zn_xO_4$ powders, Solid State Ionics 132 (2000) 63–69.
[9] B. Gillot, J.L. Baudour, F. Bouree, R. Metz, R. Legros, A. Rousset, Ionic configuration and cation distribution in cubic nickel manganite spinels $Ni_xMn_{3-x}O_4$ ($0.57 < x < 1$) in relation with thermal histories, Solid State Ionics 58 (1992) 155–161.
[10] D.B. Ghare, A.P.B. Sinha, Electrical and magnetic properties of zinc–nickel manganites, J. Phys. Chem. Solids 29 (1968) 885–894.
[11] A.J. Moulson, J.M. Herbert, Electroceramics, second ed., John Wiley & Sons, UK, 2003, pp. 160–166.